Methyl Methacrylate Synthesis: Thermodynamic Analysis for Oxidative Esterification of Methacrolein and Aldol Condensation of Methyl Acetate

Yanan Guan[a,†], Hongqin Ma[a,†], Wenyao Chen[a,*], Maoshuai Li[b], Gang Qian[a], De Chen[c], Xinggui Zhou[a], Xuezhi Duan[a,*]

[a]*State Key Laboratory of Chemical Engineering, East China University of Science and Technology, 130 Meilong Road, Shanghai 200237, China*

[b]*Key Laboratory for Green Chemical Technology of Ministry of Education, Collaborative Innovation Center of Chemical Science and Engineering, School of Chemical Engineering & Technology, Tianjin University, Tianjin 300350, China*

[c]*Department of Chemical Engineering, Norwegian University of Science and Technology, N-7491 Trondheim, Norway*

[†]These authors contributed equally to this work.

[*]To whom correspondence should be addressed. Tel.:+86-21-64250937; Email: wenyao.chen@ecust.edu.cn; xzduan@ecust.edu.cn.

ABSTRACT: Methyl methacrylate (MMA) as a specialty monomer of polymers has motivated industry to develop clean and sustainable technologies for its production. Herein, a comprehensive thermodynamic analysis of MMA production from petroleum-based and coal/biomass-based resources is conducted through the Gibbs free energy minimization method. For the petroleum-based route via oxidative esterification of methacrolein (MAL), the production of MMA is sensitive to the composition of methanol (MeOH) and O_2 in the feed, but insensitive to the reaction temperature and pressure. For the coal/biomass-based route via aldol condensation of methyl acetate (MeOAc), the medium temperature (350-400 ^oC) and large MeOH/MeOAc ratio (>2) give rise to the efficient production of MMA. Hence, significant improvements in the MMA yield could be achieved by optimizing the reaction conditions, which could almost reach the maximal value theoretically of 1.0 mol from per mole of MAL or MeOAc. This study would shed new lights on the thermodynamics of MMA production, which paves a foundation for the development of new process at the industrial scale.

1. INTRODUCTION

Methyl methacrylate (MMA) has emerged as an important industrial monomer, which is widely used for the production of poly (methyl methacrylate) (PMMA) and methyl methacrylate-butadiene-styrene copolymer (MBS).[1-3] Traditionally, MMA is mainly produced by the acetone cyanohydrin (ACH) process (Figure 1) in the cost of massive toxic hydrogen cyanide as feed and environmentally detrimental coproduction of ammonium sulfate.[4-6] As an alternative, a much more safe and environmentally friendly process has gained considerable attraction, involving the oxidation of methacrolein (MAL) to produce methacrylic acid (MAA) followed by the esterification with methanol, or oxidative esterification of MAL with oxygen and methanol to directly produce MMA (Figure 1).[7-9] So far, many metal catalysts have been tested for this reaction, among which Pd-based and Au-based catalysts demonstrate relatively high catalytic activity.[10-14] However, apart from the design and preparation of highly selective catalysts, the wide application of this process is still limited by the excess usage of methanol, the production of various byproducts, and high energy consumption as a result of long reaction time.[15,16] Hence, precise screening and optimization of the reaction parameters, including temperature, pressure and feed composition, are very crucial yet challenging to achieve the highly efficient conversion of MAL into MMA.

On the other hand, as indicated above, the MAL is a typical downstream product of the petroleum industry, which is sensitive to the supply and price of petroleum.[17,18] Hence, with the depletion of petroleum, continuous efforts have been devoted to designing and developing new process for the production of MMA from other resources, such as coal and biomass.[1] Based on the molecular structure of MMA, it can be made up of the unit of methyl acetate (MeOAc), as

well as its derivatives, e.g., methyl acrylate (MA) and methyl propionate (MP), which are the typical products of coal/biomass chemical industry.[19,20] In principle, the aldol condensation of MeOAc with formaldehyde (FA) would produce MA, which could further undergo hydrogenation to MP and then aldol condensation to MMA (Figure 1). Although many catalysts (e.g., V_2O_5, P_2O_5, Cs and La) have been developed for the first step to produce MA from MeOAc,[21-25] the process based on it to produce MMA has not been reported in previous study as best as we know, opening up new opportunities for the synthesis of MMA from coal/biomass resources. Moreover, considering the dehydrogenation of methanol (MeOH) to produce both FA and H_2 as the main reactant for the aldol condensation and hydrogenation,[26,27] it is reasonable to assume that the MeOAc could react with MeOH to directly produce MMA through a one-step process (Figure 1). Hence, according to the above discussion, it remains an open question on the possibility of MeOAc reacting with FA and H_2, or MeOH to directly produce MMA.

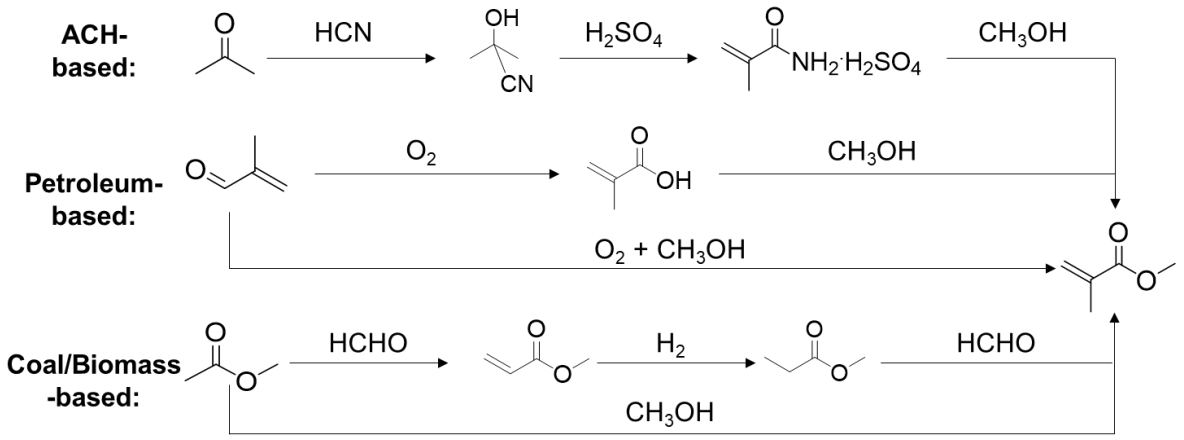

Figure 1. The ACH-based, petroleum-based and coal/biomass-based routes for the production of methyl methacrylate (MMA).

Thermodynamics is a useful tool in the design and optimization of chemical process, enabling the prediction of the reaction direction as well as the final state of the system given infinite time. Accordingly, thermodynamic equilibrium calculations based on the Gibbs free energy minimization allow us to evaluate the possibility of reactions to proceed in terms of their endothermicity/exothermicity (ΔH), the thermodynamically favorable products in terms of their selectivity and yield, and the influences of reaction parameters, including temperature, pressure, and feed compositions. To this point, for the production of MMA, the Gibbs free energy minimization method could be employed to understand the excess usage of methanol and the production of various byproducts from MAL, as well as the possibility and degree from MeOAc. However, few thermodynamics equilibrium analysis on the production of MMA based on these two routes has been done previously, which may cause the reaction parameters in experiment far from the optimal conditions. Hence, it is highly desirable to conduct a systematic thermodynamics equilibrium calculation over these two routes for a comparison, and thus guiding the optimization of operation parameters for the efficient production of MMA.

In this work, we conducted systematic thermodynamic analysis and comparison on the synthesis of MMA over the above petroleum-based and coal/biomass-based routes by using the total Gibbs free energy minimization method. The enthalpy ($\Delta_r H_T^\theta$), entropy ($\Delta_r S_T^\theta$) and Gibbs free energy ($\Delta_r G_T^\theta$) of the main and side reaction pathways were firstly calculated, yielding the reaction equilibrium constants at different temperatures. Based on which, the influences of reaction parameters, including temperature, pressure and feed composition, were respectively investigated for these two routes. As a result, the optimal operation conditions would be provided, which can guide the design and development of efficient production of MMA in

practical application.

2. METHODOLOGY

Herein, the Gibbs free energy minimization method was employed to calculate the equilibrium composition of reaction system.[28] Typically, the total Gibbs free energy of the whole system for species i could be correlated with the temperature and pressure through:

$$G_T = \sum_{i=1}^{m} n_i \mu_i = \sum_{i=1}^{m} n_i \mu_i^0 + RT \sum_{i=1}^{m} n_i \ln \frac{f_i}{f_i^0} \quad (1)$$

in which n_i, μ_i and f_i are the moles, chemical potential and fugacity of species i, respectively. The R and T are the molar gas constant and system temperature, respectively. For the reaction equilibrium, f_i can be calculated by:

$$f_i = \varphi_i y_i p \quad (2)$$

where φ_i is the fugacity of species i and obtained from equation of state. The y_i and p are the mole fraction of species i and pressure, respectively. On the other hand, the minimization of total Gibbs free energy of the whole system is subject to mass balance constraints:

$$\mu_i + \sum_{j=0}^{k} \lambda_i a_{ji} = 0 \quad (3)$$

where λ and α_{ji} are the Lagrange multiplier and the number of atoms of element j in species i, respectively. Hence, a combination of Eqs. 1-3 gives Eq. 4 as:

$$\sum_{i=1}^{m} n_i (\mu_i^0 + RT \ln \frac{\varphi_i y_i p}{f_i^0} + \sum_{j=0}^{k} \lambda_i a_{ji}) = 0 \quad (4)$$

A literature review cited above indicates the possible occurrence of independent reactions as following:

Oxidation of MAL to produce MAA:

$MAL + 1/2O_2 \rightarrow MAA$ R1

Esterification of MAA with MeOH to produce MMA:

$MAA + MeOH \rightarrow MMA + H_2O$ R2

Oxidative esterification of MAL with oxygen and methanol to directly produce MMA:

$MAL + MeOH + 1/2O_2 \rightarrow MMA + H_2O$ R3

Oxidative esterification MeOH to produce methyl formate (MF):

$2MeOH + O_2 \rightarrow MF + 2H_2O$ R4

Aldol condensation of MeOAc with FA to produce MA:

$MeOAc + FA \rightarrow MA + H_2O$ R5

Hydrogenation of MA to produce MP:

$MA + H_2 \rightarrow MP$ R6

Aldol condensation of MP with FA to produce MMA:

$MP + FA \rightarrow MMA + H_2O$ R7

Dehydrogenation of MeOH to produce H_2 and FA:

$MeOH \rightarrow H_2 + FA$ R8

Aldol condensation and hydrogenation of MeOAc with MeOH to produce MMA:

$MeOAc + 2\ MeOH \rightarrow MMA + H_2 + 2H_2O$ R9

As a result, the equilibrium compositions of the whole system based on the above reactions can be calculated as a function of temperature, pressure and feed composition based on the Gibbs free-energy minimization module (RGIBBS Gibbs reactor) within the ASPEN PLUS computer software. The physicochemical parameters of chemical compound involved in this study were retrieved from the ASPEN PLUS Pure Component Data Base. The UNIQUAC and

SRK equation of states were employed for the calculation of petroleum-based route (R1-R4) and coal/biomass-based route (R5-R9), respectively.

It is worth to note that several complications emerged in our preliminary calculations: the amounts of generated MAL and MP are higher than those of MAL and MeOAc in the feed for the petroleum-based route and coal/biomass-based route, respectively, which could be interpreted as the "unrestricted" free-energy minimization calculations. To avoid this problem, it is necessary to restrict and specify the stoichiometric coefficients for the above reactions. Generally, the number of linearly independent reactions should be equal to the difference between the number of products and that of atoms within the system.[29] Hence, in order to satisfy the material balances, another two linearly independent reactions were further considered as:

$$4\,MeOH + O_2 \rightarrow MAL + 5H_2O \qquad R10$$

$$4\,MeOH \rightarrow MP + 2H_2O + 2H_2 \qquad R11$$

in which R10 and R11 were postulated for the petroleum-based route (R1-R4) and coal-based route (R5-R9), respectively.

3. RESULTS AND DISCUSSION

3.1. Petroleum-based Route to Produce MMA.

According to the above discussion on the petroleum-based route, the MMA could be synthesized via either two-step (oxidation followed by esterification) or one-step (oxidative esterification) pathway as shown in Figure 2. Moreover, for the one-step oxidative esterification, the coexistence of oxygen and MeOH in the feed could result in the oxidative esterification of MeOH to produce methyl formate (MF). Hence, the thermodynamic calculation for this route

mainly involves the chemical components such as MAL, MAA, MMA, MeOH, O_2 and MF, in which the MAA and MF are the undesirable products. Correspondingly, Table S1 lists the thermodynamic parameters, including $\Delta_f H_{298.15}^{\theta}$, $S_{298.15}^{\theta}$ and heat capacity, for these species.[30] As a result, the enthalpy of reaction ($\Delta_r H_{298.15}^{\theta}$) for R1-R4 could be calculated as shown in Figure 2. Obviously, the reaction enthalpy of R1, R3 and R4 is much lower than that of R2. In other words, this indicates that the R1, R3 and R4 are more thermodynamically favorable compared with the R2 at relatively low temperature. As a result, the reaction equilibrium of the two-step pathway could be mainly limited by the esterification of MAA (R2) with the lowest equilibrium constant. On the contrary, for the one-step pathway, the similar reaction enthalpy for the R3 and R4 indicates that the competition between the main reaction R3 and side reaction R4 is important to achieve high yield of MMA from the point view of thermodynamics.

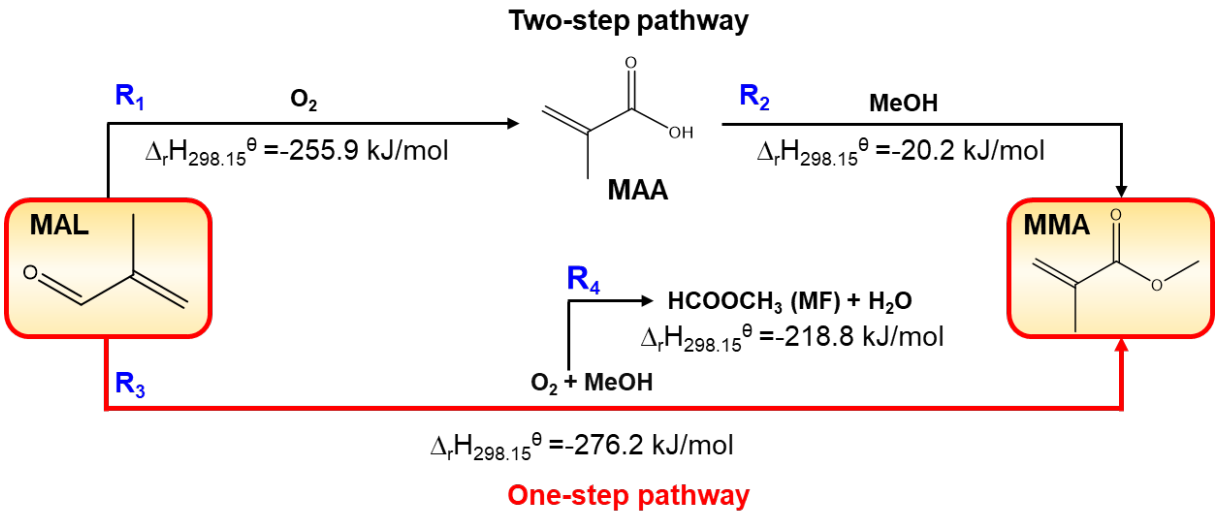

Figure 2. The thermodynamic calculation on the petroleum-based route to produce MMA from MAL.

Moreover, the standard enthalpy ($\Delta_f H_T^{\theta}$) and entropy (S_T^{θ}) of these species could be respectively calculated as a function of reaction temperature based on *Eqs. 5* and *6*:

$$\Delta_f H_T^\theta = \Delta_f H_{298.15}^\theta + \int_{298.15}^{T} c_p dT \quad (5)$$

$$S_T^\theta = S_{298.15}^\theta + \int_{298.15}^{T} \frac{c_p}{T} dT \quad (6)$$

in which c_p could be calculated according to:

$$c_p = A + B*T + C*T^2 + D*T^3 \quad (7)$$

Hence, the enthalpy ($\Delta_r H_T^\theta$), entropy ($\Delta_r S_T^\theta$) and Gibbs free energy ($\Delta_r G_T^\theta$) of formation for R1-R4 could be calculated as shown Table S2-S5, based on which the reaction equilibrium constant (K^θ) could be further obtained as shown in Figure 3.

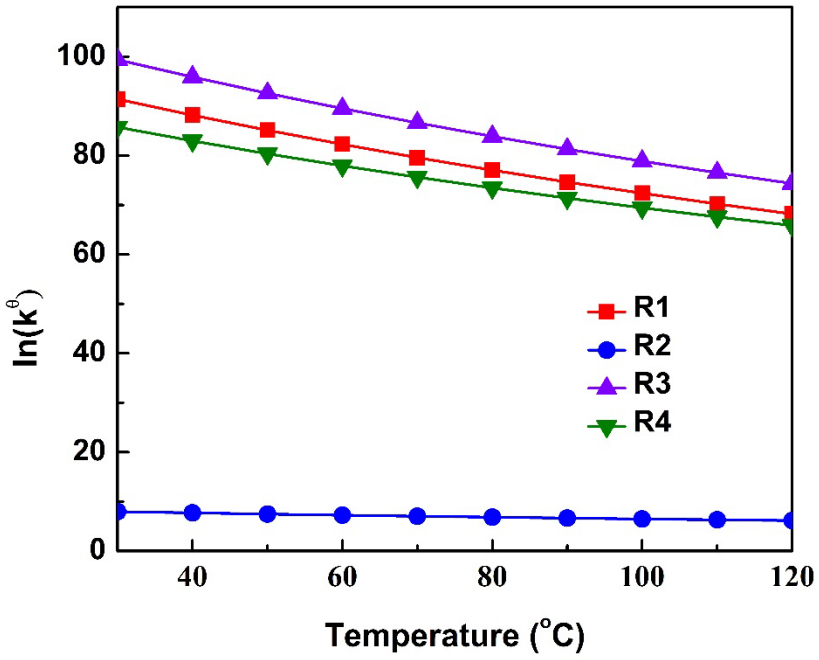

Figure 3. Equilibrium constant as a function of reaction temperature for R1-R4.

It is obvious that the equilibrium constant of R2 is much smaller compared with the other three reactions at the typical reaction condition of temperature (30-120 °C). On the contrary, the direct oxidative esterification of MAL to MMA, i.e., R3, appears to be the most

thermodynamically favorable reaction with the largest equilibrium constant. Meanwhile, although the equilibrium constants for these four reactions decrease with the temperature, their values are still large enough for the conversion of MAL into MMA. Based on the above discussion, from the point view of thermodynamics, it can be deduced that the one-step pathway could give rise to much higher yield of MMA compared with the two-step pathway.

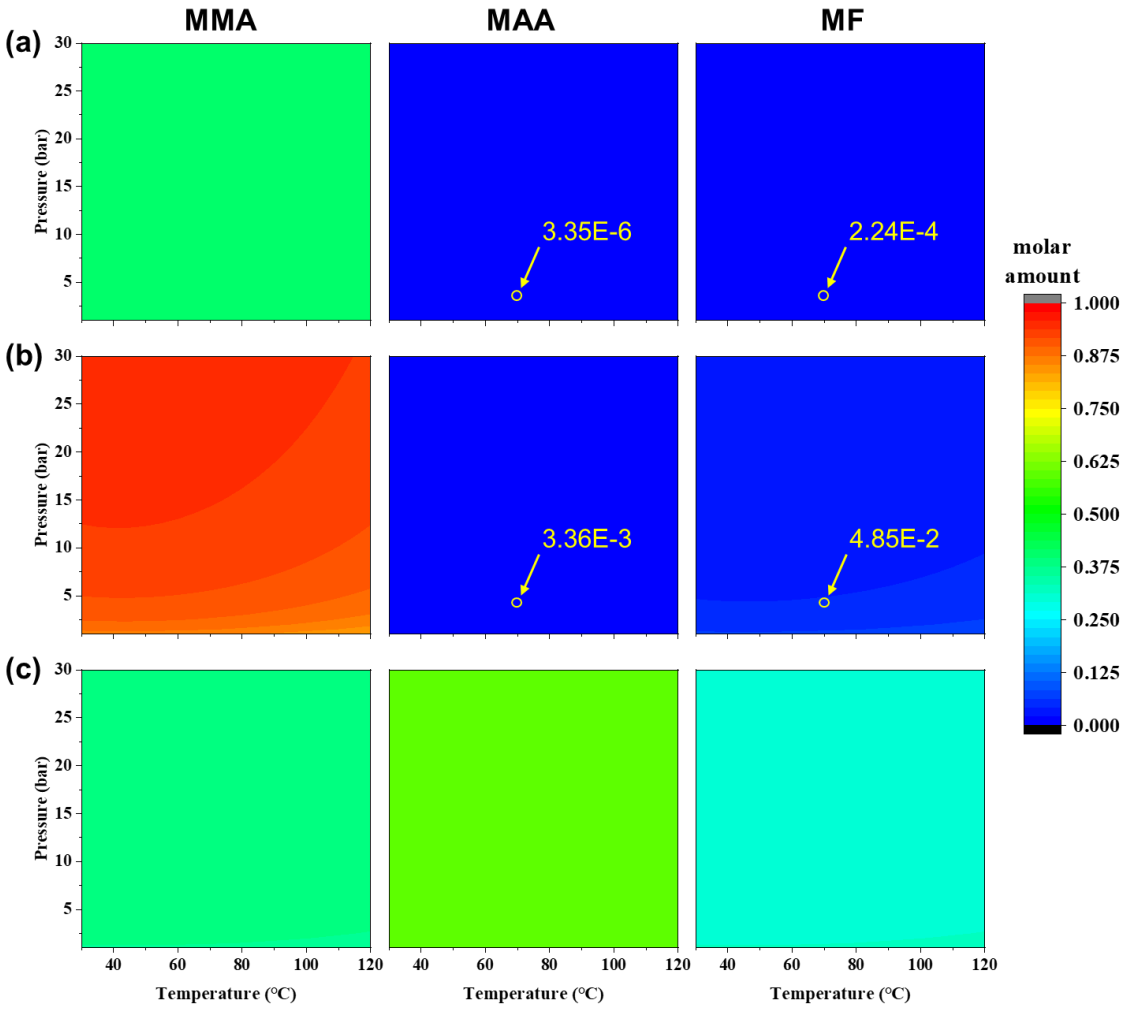

Figure 4. The molar amounts of MMA, MAA and MF produced from per mole of MAL as a function of temperature and pressure at different ratios of O_2/MAL: (a) O_2/MAL = 0.2, (b) O_2/MAL = 0.5, and (c) O_2/MAL = 0.8.

The influences of the temperature, pressure and feed composition were further investigated by thermodynamic simulation using the Gibbs free energy minimization method. Figure 4 presents the moles of MMA, MAA and MF produced from per mole of MAL as a function of temperature, pressure and O_2/MAL ratio under the same MeOH/MAL ratio of 1, which is the stoichiometric molar ratio of oxidative esterification. It can be seen that not only temperature but also pressure has neglectable influences on the product distribution, in contrast to the significant influence of O_2/MAL ratio. To be more specifically, at the low O_2/MAL ratio of 0.2, the MMA appears to be the main product with 0.39 mol production from per mole of MAL in comparison to the negligible production of MAA and MF. This could be interpreted as the shortage of O_2 for the oxidation of MAL into MAA and oxidative esterification of MeOH into MF, respectively.

With the increase of O_2/MAL ratio to 0.5, a sharp increment of MMA amount can be observed, which almost reaches the maximal value theoretically of 1.0 mol from per mole of MAL. It is worth to note that the O_2/MAL ratio of 0.5 is the stoichiometric molar ratio for the oxidative esterification of MAL, which will facilitate its conversion. Moreover, in light of the largest equilibrium constant of R3, the converted MAL prefers to generate MMA rather than MAA and MF, giving rise to the highest yield of MMA as shown in Figure 4. At this condition, the influences of the temperature and pressure become visible. As can be seen that, the lower temperature and higher pressure would further promote the yield of MMA, due to the exothermicity and molecular number reduction of R3. Unexpectedly, as shown in Figure 4, further increasing the O_2/MAL ratio to 0.8 would lower the molar amount of MMA to 0.38. This is because the excess of O_2 would promote the oxidative esterification of MeOH into MF

(R4). Considering that the ratio of MeOH/MAL in the feed is 1, the consumption of MeOH for R4 will result in the insufficient MeOH for the conversion of MAL into MMA (R3).

Based on the above discussion, it can be seen that both the ratios of O_2/MAL and MeOH/MAL have significant influences on the product distribution for MAL conversion. Considering the limited influences of temperature and pressure, 70 ^oC and 3 bar, as typical experimental reaction conditions in the previous work,[7] were chosen for this study, and the results are shown in Figure 5. It is obvious that the total amounts of MMA, MAA and MF increase with the ratio of O_2/MAL at any ratio of MeOH/MAL in the range of 0.5-20, ascribed to the promotional effect of O_2 on MAL conversion. Specifically, at the lower MeOH/MAL ratio (<2.50), the two-step pathway is the main reaction route for the MMA production. Under this condition, the insufficient O_2 (O_2/MAL<0.15) results in the lower MAL conversion as well as MMA, MAA production; the excess O_2 (O_2/MAL>0.63) results in the large production of MAA as the product of MAL oxidation. Hence, the appropriate amount of O_2 (0.15<O_2/MAL<0.63) would promote the production of MMA as the main product, although its amount is still unsatisfied. With the increase of MeOH/MAL ratio (>2.50), the main reaction route shifts from the two-step pathway to one-step pathway, and the production of MAA is inhibited. Under this condition, the amounts of MMA and MF production continuously increase with the ratio of O_2/MAL, especially for the MMA. It can be seen that the amount of MMA is close to the maximal value theoretically once the O_2/MAL ratio exceeds the stoichiometric ratio of 0.5. Based on the above discussion, the optimal MeOH/MAL and O_2/MAL ratios for the MMA production should be larger than 2.5 and 0.5, respectively.

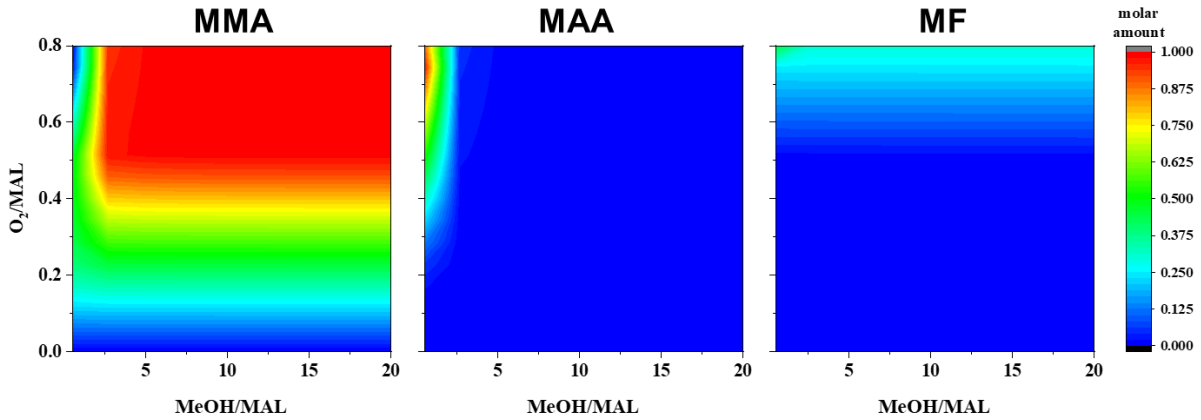

Figure 5. The molar amounts of MMA, MAA and MF produced from per mole of MAL at 70 °C and 3 bar as a function of the ratios of O_2/MAL and MeOH/MAL.

To this end, both the temperature and pressure are found to have limited influences on the product distribution. On the contrary, it is significantly affected by the ratio of either MeOH/MAL or O_2/MAL. In other words, the higher compositions of MeOH and O_2 with respect to MAL in the feed, the higher composition of desirable MMA in the product. A case adopted from the literature was also studied here to verify the effectiveness of our calculation. Specifically, it is found that, under the experimental condition (70 °C, MeOH/MAL=8, 0.3 MPa O_2), the conversion of MAL and the yield of MMA for direct oxidative esterification over Au/La_2O_3 catalyst could reach 92% and 91%,[7] which is close to the theoretical MAL conversion of 99.5% and MMA yield of 99.2%, respectively. Hence, the consistence between the experimental data with the theoretically thermodynamic calculation further confirms that this reaction is mainly governed by kinetics instead of thermodynamics. Moreover, for the two-step oxidation then esterification pathway, the highest MAL conversion and MAA yield have been reported as 83% and 77% over the $Cs(NH_4)_xH_{3-x}PMo_{11}VO_{40}$ catalyst, respectively.[31] As a result,

the maximum MMA yield based on MAL for this kind catalyst is reasonably lower than 77%. Hence, compared with the two-step pathway, the one-step pathway exhibits not only high energy efficiency and low environmental footprint, but also high catalytic performance, which makes it more attractive for commercial production of MMA.

3.2. Coal/Biomass-based Route to Produce MMA.

Based on the above discussion on coal/biomass-based route, the MMA could be synthesized from MeOAc. Typically, the MeOAc could be produced by the esterification of acetic acid and MeOH, which are the typical products of coal and biomass chemical industry. Hence, as shown in Figure 6, the as-obtained MeOAc could further react with FA and H_2 to produce MMA via a three-step pathway: aldol condensation with FA to produce MA, followed by hydrogenation to MP, and lastly aldol condensation with another FA to MMA. Moreover, considering the complexity of the above process, it remains an open question whether the MeOAc could react with the MeOH, as the origin of FA and H_2, to direct produce MMA via a one-step pathway.

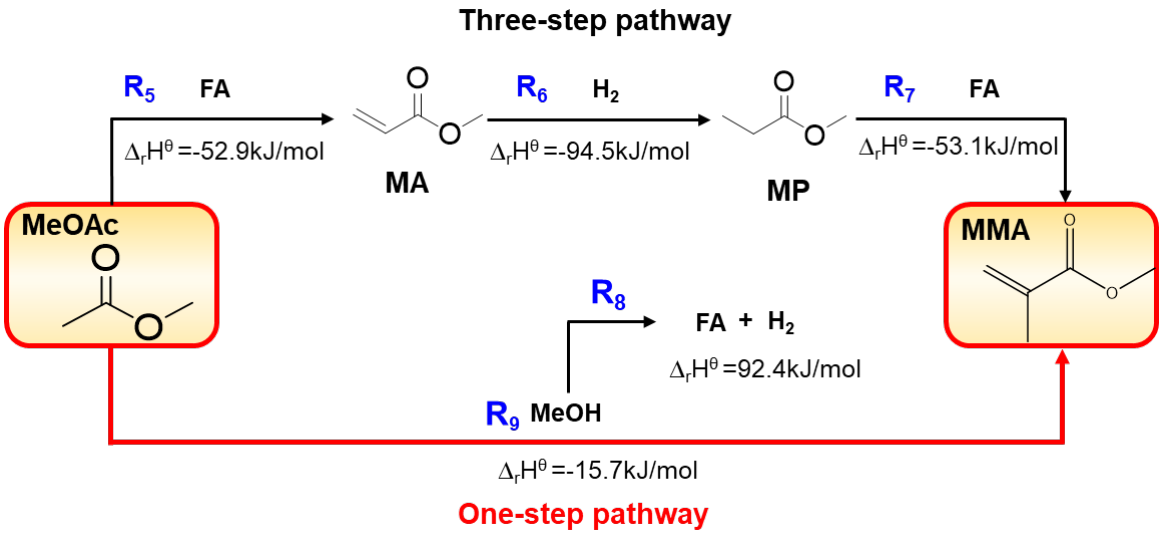

Figure 6. The thermodynamic calculation on the coal/biomass-based route to produce MMA from MeOAc.

The thermodynamic calculation for this route mainly involves the chemical components such as MeOAc, MA, MP, MMA, MeOH, FA and H_2, in which the MA and MP are the undesirable products. Correspondingly, Table S6 lists the thermodynamic parameters, including $\Delta_f H_{298.15}^{\theta}$, $S_{298.15}^{\theta}$ and heat capacity, for these species.[30] Consequently, the enthalpy ($\Delta_r H_{298.15}^{\theta}$) of formation for R5-R9 could be calculated as shown in Figure 6. Obviously, the R5, R6 and R7 emerge as exothermic reactions with the negative enthalpy of reaction, while the R8 as endothermic reaction with the positive enthalpy of reaction. In comparison, the absolute enthalpy of reaction for R9 is the lowest among these reactions. Moreover, to incorporate the influences of the reaction temperature, the standard enthalpy ($\Delta_f H_T^{\theta}$) and entropy (S_T^{θ}) of these species could be respectively calculated as a function of reaction temperature based on *Eqs. 5* and *6*. As a result, the enthalpy ($\Delta_r H_T^{\theta}$), entropy ($\Delta_r S_T^{\theta}$) and Gibbs free energy ($\Delta_r G_T^{\theta}$) of formation for R5-R9 could be calculated as shown in Table S7-S11, based on which the reaction equilibrium constant (K^{θ}) could be further calculated as shown in Figure 7.

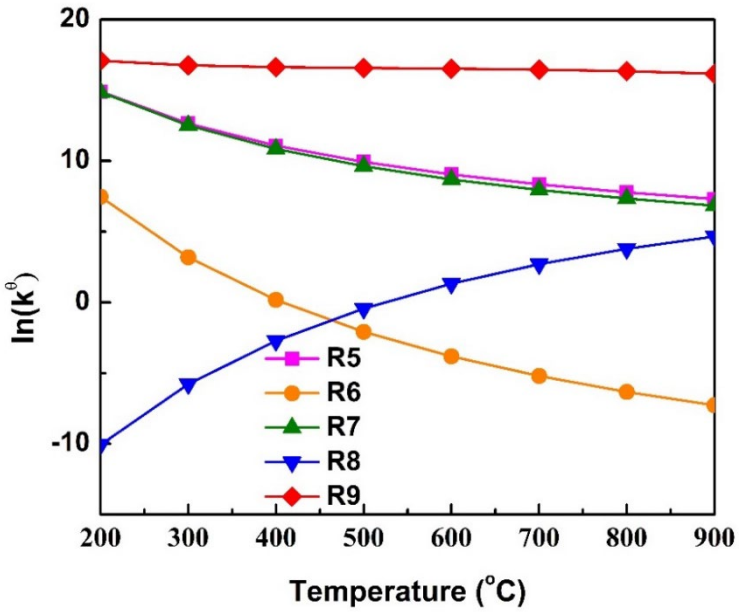

Figure 7. Equilibrium constants as a function of reaction temperature for R5-R9.

It can be seen in Figure 7 that for the three-step pathway, the reaction equilibrium constants for the R5 and R7 are much large despite of the reaction temperature change, which indicates them much more thermodynamically favorable. In contrast, the reaction equilibrium constant of R6 is highly sensitive to the change of temperature, whose Gibbs energy shifts from negative to positive value around 400 °C. This suggests that the R6 becomes thermodynamically unfavorable when the temperature exceeds 400 °C. Hence, the reaction temperature should be no more than 400 °C to ensure the hydrogenation of MA. For the one-step pathway, the equilibrium constant for the dehydrogenation of MeOH (R8) increases with the reaction temperature, which can serve as the resource of FA and H_2 for the three-step pathway. Hence, the reaction temperature should be no less than 300 °C to ensure the production of FA and H_2 for the three-step pathway. Based on the above discussion, compared with the petroleum-based route, it is found that the reaction temperature has a significant influence on the coal/biomass-based route, which should exist an optimal value for MMA production.

Figure 8 presents the molar amounts of MMA, MA and MP produced from per mole of MeOAc as a function of temperature, pressure and MeOH/MeOAc ratio. Figure 8a demonstrates the influences of the temperature and pressure on the product distribution. It can be seen that the MMA remains the main product at low temperature, whose amount increases with the temperature. This is because at the low temperature, the one-step pathway is the main reaction, and the three-step pathway is inhibited due to the limited supply of FA and H_2 from MeOH dehydrogenation (R8). Considering that the molecular number of the one-step pathway increases, the pressure has a negative influence on the conversion of MeOAc into MMA. With the rise of temperature, more FA and H_2 would be produced from MeOH dehydrogenation (R8)

with the enlarged reaction equilibrium constant. However, further increasing temperature would inhibit the hydrogenation of MA to MP (R6) due to its lowest reaction equilibrium constant at high temperature, although massive FA and H_2 are produced from MeOH (R8). As a result, the MA instead of the MMA becomes the main product at high reaction temperature.

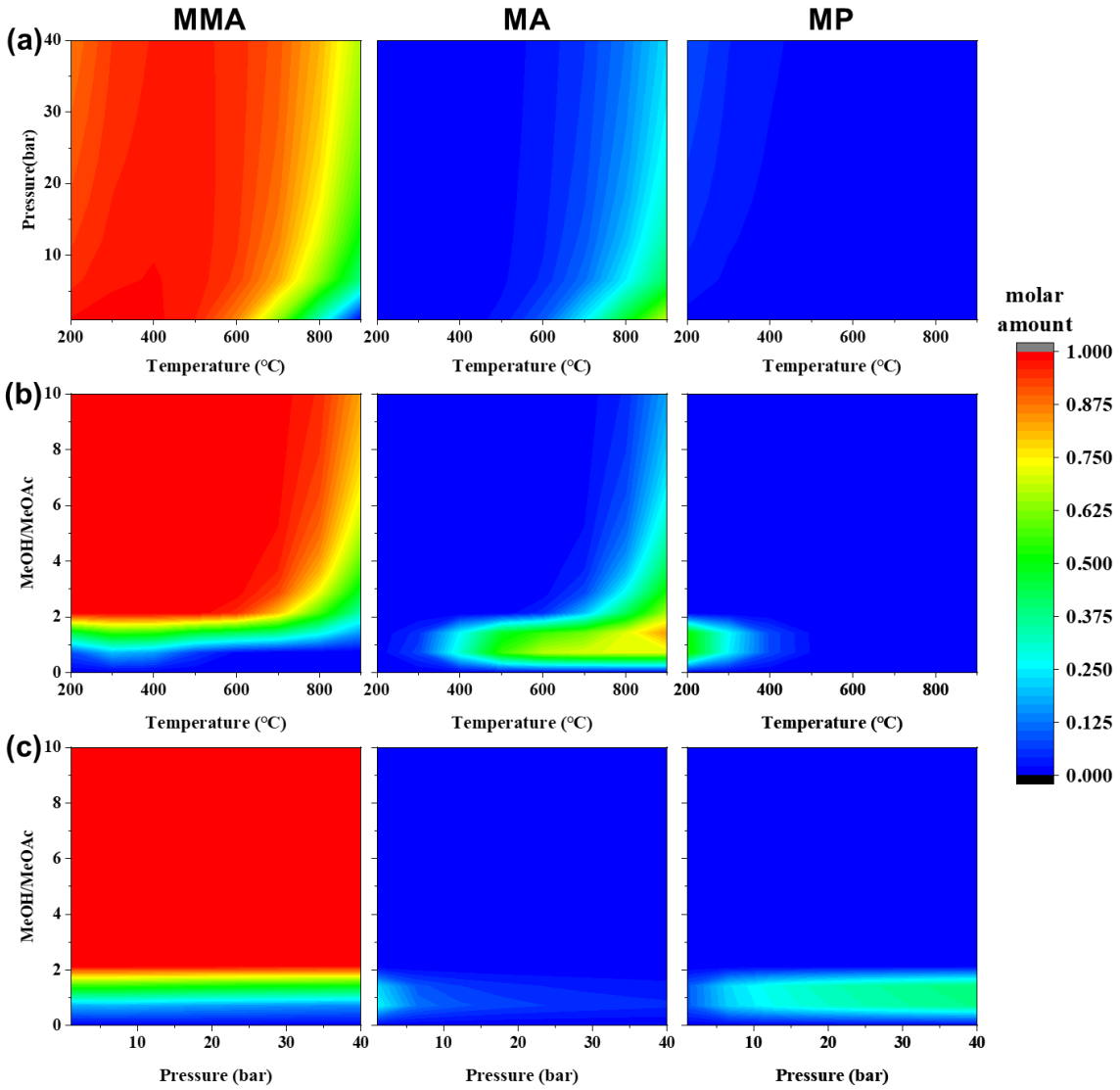

Figure 8. The molar amounts of MMA, MA and MP produced from per mole of MeOAc as a function of (a) temperature and pressure (MeOH/MeOAc=2), (b) MeOH/MeOAc and temperature (pressure=1 bar), and (c) MeOH/MeOAc and pressure (temperature=385 °C).

Apart from temperature and pressure, Figure 8b demonstrates the influence of the MeOH/MeOAc ratio on the product distribution, which can be divided into three domains. At low MeOH/MeOAc ratio less than 1, the production of MMA is negligible despite of the temperature change, ascribed to the serious shortage of MeOH for R9. Moreover, a few MP (R6) and MA (R5) are produced from MeOAc at low and high temperature within this domain, respectively, due to the increased supply of FA and H_2 by R8. At medium MeOH/MeOAc ratio between 1 and 2, both MMA and MA could be produced with small amount. On the contrary, at high MeOH/MeOAc ratio larger than 2, there is an increase in the amount of MMA production. Within the domain, because the MeOH/MeOAc ratio is excess than the stoichiometric molar ratio (2) and the large reaction equilibrium of R9, the production of MMA is highly promoted and almost reaching the maximal value theoretically of 1.0 mol from per mole of MeOAc. Based on the above discussion, it can be deduced that the higher MeOH/MeOAc ratio, the larger amount of MMA production.

Furthermore, Figure 8c gives the influences of pressure and MeOH/MeOAc ratio on the product distribution. It is obvious that the productions of MA and MP are more significantly affected by pressure than that of MMA. Because the hydrogenation of MA to MP is a molecular number reduction reaction, the high pressure would promote the conversion of MA into MP. Hence, a combination of temperature, pressure and MeOH/MeOAc ratio influences suggests that the medium temperature (350-400 ^{o}C) and large MeOH/MeOAc ratio (>2) would highly promote the MMA production, while negligible influence of pressure. Notably, although MeOH dehydrogenation (R8) is significantly influenced by thermodynamic constraints with the lowest equilibrium constant (K<0.07), the MeOAc could be still almost completely converted into

MMA as shown in Figure 8. This could be interpreted as the produced H_2 of R8 would be soon consumed by the hydrogenation of MA (R6), which circumvents the thermodynamic bottlenecks of MeOH dehydrogenation and renders the production of MMA more feasible. Thus, from the point view of thermodynamics, the coal/biomass-based route appears to be a promising approach to produce MMA. However, as best as we know, few experimental and kinetic studies have been conducted over this route. Considering that Cu- and TiO_2-based catalysts exhibit high catalytic activity for the dehydrogenation/hydrogenation and aldol condensation of unsaturated carbonyl compounds, respectively,[32] it is highly desirable to prepare the bifunctional Cu-TiO_2 catalyst to achieve their synergy for the efficient production of MMA based on the coal/biomass resources.

4. CONCLUSION

In summary, we have systematically studied the thermodynamics for the synthesis of MMA over the two routes, namely, petroleum-based route and coal/biomass-based route. The total Gibbs free energy minimization method has been employed to investigate the influences of the temperature, pressure, and feed composition on the product distributions. For the petroleum-based route via the oxidation and esterification of MAL, the resultant product distribution is highly sensitive to the ratios of MeOH/MAL and O_2/MAL in the feed, while insensitive to the reaction temperature and pressure. It is found that increasing the compositions of MeOH and O_2 with respect to MAL in the feed would promote the generation of MMA. For the coal/biomass-based route via the aldol condensation and hydrogenation of MeOAc, the resultant product distribution is strongly affected by the temperature and the ratio of

MeOH/MeOAc, in comparison with the negligible influence of reaction pressure. It is revealed that the medium temperature (350-400 ^{o}C) and large MeOH/MeOAc ratio (>2) would facilitate the production of MMA. For both two routes, the yield of MMA could almost reach the maximal value theoretically of 1.0 mol from per mole of MAL or MeOAc under the optimized reaction conditions, and the design of highly active catalyst could be the key to achieve efficient production of MMA in industry.

Acknowledgments

This work was financially supported by the Natural Science Foundation of China (21922803 and 21776077), the Shanghai Natural Science Foundation (17ZR1407300 and 17ZR1407500), the China Postdoctoral Science Foundation (BX20190116), the Program for Professor of Special Appointment (Eastern Scholar) at Shanghai Institutions of Higher Learning, the Shanghai Rising-Star Program (17QA1401200), the State Key Laboratory of Organic-Inorganic Composites (oic-201801007), 111 Project of the Ministry of Education of China (B08021) and the Open Project of State Key Laboratory of Chemical Engineering (SKLChe-15C03).

References

[1] Mahboub, M. J. D.; Dubois, J. L.; Cavani, F.; Rostamizadeh, M.; Patience, G. S. Catalysis for the synthesis of methacrylic acid and methyl methacrylate. *Chem. Soc. Rev.* **2018**, 47 (20), 7703-7738.

[2] Nagai, K. New developments in the production of methyl methacrylate. *Appl. Catal. A: General* **2001**, 221 (1-2), 367-377.

[3] Ali, U.; Karim, K. J. B. A.; Buang, N. A. A review of the properties and applications of poly (methyl methacrylate)(PMMA). *Polym. Rev.* **2015**, 55 (4), 678-705.

[4] Tai, J.; Davis, R. J. Synthesis of methacrylic acid by aldol condensation of propionic acid with formaldehyde over acid-base bifunctional catalysts. *Catal. Today* **2007**, 123 (1-4), 42-49.

[5] Nguyen, N. H.; Kendell, S.; Le Minh, C.; Brown, T. Mechanistic investigation into the rearrangement of lactone into methacrylic acid over phosphomolybdic acid catalyst. *Catal. Lett.* **2010**, 136 (1-2), 28-34.

[6] McFarlane, A. R.; Geller, H.; Silverwood, I. P.; Cooper, R. I.; Watkin, D. J.; Parker, S. F.; Winfield, J. M.; Lennon, D. The application of inelastic neutron scattering to investigate the interaction of methyl propanoate with silica. *Phys. Chem. Chem. Phys.* **2016**, 18 (26), 17210-17216.

[7] Paul, B.; Khatun, R.; Sharma, S. K.; Adak, S.; Singh, G.; Das, D.; Siddiqui, N.; Bhandari, S.; Joshi, V.; Sasaki, T.; Bal, R. Fabrication of Au nanoparticles supported on one-dimensional La_2O_3 nanorods for selective esterification of methacrolein to methyl methacrylate with molecular oxygen. *ACS Sustain. Chem. Eng.* **2019**, 7 (4), 3982-3994.

[8] Diao, Y.; He, H.; Yang, P.; Wang, L.; Zhang, S. Optimizing the structure of supported Pd catalyst for direct oxidative esterification of methacrolein with methanol. *Chem. Eng. Sci.* **2015**, 135, 128-136.

[9] Han, J.; Zhang, S.; Li, Y.; Yan, R. Multi-scale promoting effects of lead for palladium catalyzed aerobic oxidative coupling of methylacrolein with methanol. *Catal. Sci. Techno.* **2015**, 5 (4), 2076-2080.

[10] Wang, B.; Sun, W.; Zhu, J.; Ran, W.; Chen, S. Pd-Pb/SDB bimetallic catalysts for the direct

oxidative esterification of methacrolein to methyl methacrylate. *Ind. Eng. Chem. Res.* **2012**, 51 (46), 15004-15010.

[11] Wang, B.; Li, H.; Zhu, J.; Sun, W.; Chen, S. Preparation and characterization of mono-/multi-metallic hydrophobic catalysts for the oxidative esterification of methacrolein to methyl methacrylate. *J. Mol. Catal. A: Chem.* **2013**, 379, 322-326.

[12] Diao, Y.; Yang, P.; Yan, R.; Jiang, L.; Wang, L.; Zhang, H.; Li, C.; Li, Z.; Zhang, S. Deactivation and regeneration of the supported bimetallic Pd-Pb catalyst in direct oxidative esterification of methacrolein with methanol. *Appl. Catal. B: Environ.* **2013**, 142, 329-336.

[13] Jiang, L.; Diao, Y.; Han, J.; Yan, R.; Zhang, X.; Zhang, S. MgO-SBA-15 supported Pd-Pb catalysts for oxidative esterification of methacrolein with methanol to methyl methacrylate. *Chin. J. Chem. Eng.* **2014**, 22 (10), 1098-1104.

[14] Li, Y.; Wang, L.; Yan, R.; Han, J.; Zhang, S. Promoting effects of MgO, $(NH_4)_2SO_4$ or MoO_3 modification in oxidative esterification of methacrolein over $Au/Ce_{0.6}Zr_{0.4}O_2$-based catalysts. *Catal. Sci. Techno.* **2016**, 6 (14), 5453-5463.

[15] Yamamatsu, S.; Yamaguchi, T.; Yokota, K.; Nagano, O.; Chono, M.; Aoshima, A. Development of catalyst technology for producing methyl methacrylate (MMA) by direct methyl esterification. *Catal. Surv. Asia* **2010**, 14 (3-4), 124-131.

[16] Gao, J.; Fan, G.; Yang, L.; Cao, X.; Zhang, P.; Li, F. Oxidative esterification of methacrolein to methyl methacrylate over gold nanoparticles on hydroxyapatite. *ChemCatChem* **2017**, 9 (7), 1230-1241.

[17] Gaigneaux, E. M.; Genet, M. J.; Ruiz, P.; Delmon, B. Catalytic behavior of molybdenum suboxides in the selective oxidation of isobutene to methacrolein. *J. Phys. Chem. B* **2000**, 104

(24), 5724-5737.

[18] Liu, H.; Gaigneaux, E. M.; Imoto, H.; Shido, T.; Iwasawa, Y. Performance and characterization of novel Re-Sb-O catalysts active for the selective oxidation of isobutylene to methacrolein. *J. Phys. Chem. B* **2000**, 104 (9), 2033-2043.

[19] Isikgor, F. H.; Becer, C. R. Lignocellulosic biomass: A sustainable platform for the production of bio-based chemicals and polymers. *Polym. Chem.* **2015**, 6 (25), 4497-4559.

[20] Xu, Y.; Wang, T.; Ma, L.; Zhang, Q.; Wang, L. Upgrading of liquid fuel from the vacuum pyrolysis of biomass over the Mo-Ni/γ-Al_2O_3 catalysts. *Biomass Bioenerg.* **2009**, 33 (8), 1030-1036.

[21] Zhang, G.; Zhang, H.; Yang, D.; Li, C.; Peng, Z.; Zhang, S. Catalysts, kinetics and process optimization for the synthesis of methyl acrylate over Cs-P/γ-Al_2O_3. *Catal. Sci. Techno.* **2016**, 6 (16), 6417-6430.

[22] Wang, Y; Yan, R.; Lv, Z.; Wang, H.; Wang, L.; Li, Z.; Zhang, S. Lanthanum and cesium-loaded SBA-15 catalysts for MMA synthesis by aldol condensation of methyl propionate and formaldehyde. *Catal. Lett.* **2016**, 146 (9), 1808-1818.

[23] Li, B.; Yan, R.; Wang, L.; Diao, Y.; Li, Z.; Zhang, S. SBA-15 supported cesium catalyst for methyl methacrylate synthesis via condensation of methyl propionate with formaldehyde. *Ind. Eng. Chem. Res.* **2014**, 53 (4), 1386-1394.

[24] Li, B.; Yan, R.; Wang, L.; Diao, Y.; Li, Z.; Zhang, S. Synthesis of methyl methacrylate by aldol condensation of methyl propionate with formaldehyde over acid-base bifunctional catalysts. *Catal. Lett.* **2013**, 143 (8), 829-838.

[25] Zhao, H.; Zuo, C.; Yang, D.; Li, C.; Zhang, S. Effects of support for vanadium phosphorus

oxide catalysts on vapor-phase aldol condensation of methyl acetate with formaldehyde. *Ind. Eng. Chem. Res.* **2016**, 55 (50), 12693-12702.

[26] Boucher, M. B.; Marcinkowski, M. D.; Liriano, M. L.; Murphy, C. J.; Lewis, E. A.; Jewell, A. D.; Mattera, M. F. G.; Kyriakou, G.; Flytzani-Stephanopoulos, M.; Sykes, E. C. H. Molecular-scale perspective of water-catalyzed methanol dehydrogenation to formaldehyde. *ACS Nano* **2013**, 7 (7), 6181-6187.

[27] Usachev, N. Y.; Krukovskii, I. M.; Kanaev, S. A. The nonoxidative methanol dehydrogenation to formaldehyde (A review). *Petrol. Chem.* **2004**, 44 (6), 379-394.

[28] Perry, R. H.; Green, D. W.; Maloney, J. O. Perry's Chemical Engineers' Handbook; McGraw-Hills: New York, 1997; pp 5664.

[29] Shreiber, E. H.; Mullen, J. R.; Gogate, M. R.; Spivey, J. J.; Roberts, G. W. Thermodynamics of methacrylate synthesis from methanol and a propionate. *Ind. Eng. Chem. Res.* **1996**, 35 (7), 2444-2452.

[30] Yaws, C. L. Chemical properties handbook: physical, thermodynamic, environmental, transport, safety, and health related properties for organic and inorganic chemicals; McGraw-Hill, New York, **1999**.

[31] Cao, Y. L.; Wang, L.; Zhou, L. L.; Zhang, G. J.; Xu, B. H.; Zhang, S. J. Cs $(NH_4)_xH_{3-x}PMo_{11}VO_{40}$ catalyzed selective oxidation of methacrolein to methacrylic acid: Effects of NH_4^+ on the structure and catalytic activity. *Ind. Eng. Chem. Res.* **2017**, 56 (3), 653-664.

[32] Wang, S.; Goulas, K.; Iglesia, E. Condensation and esterification reactions of alkanals, alkanones, and alkanols on TiO_2: Elementary steps, site requirements, and synergistic effects of bifunctional strategies. *J. Catal.* **2016**, 340, 302-320.

Table of Content Graphic